Spectrochimica Acta Part A: Molecular and Biomolecular Spectroscopy 223 (2019) 117325

Contents lists available at ScienceDirect

Spectrochimica Acta Part A: Molecular and Biomolecular Spectroscopy

journal homepage: www.elsevier.com/locate/saa

Aggregative ways of graphene quantum dots with nitrogen-rich edges for direct emission spectrophotometric estimation of glucose

Praveen Mishra, Badekai Ramachandra Bhat *

Catalysis and Materials Laboratory, Department of Chemistry, National Institute of Technology Karnataka, Surathkal, Mangalore 575025, Karnataka, India

ARTICLE INFO

Article history:
Received 16 April 2019
Received in revised form 26 June 2019
Accepted 28 June 2019
Available online 29 June 2019

Keywords:
Graphene quantum dots
Photoluminescence
UV–vis absorption
Quantitative determination

ABSTRACT

We report a facile one step in-situ synthesis of amino-functionalized graphene dots. These quantum dots were employed for the detection of glucose in both standard aqueous solutions and commercially available fruit juice to assess its practicability. The characterization of the quantum dots revealed that they were decorated with amine functionality. Additionally, the interaction between glucose and amine functionalized graphene quantum dots gave enhancement in the UV–vis absorption and photoluminescence (PL) due to aggregation of quantum dots via glucose link. Therefore, the quantum dots were able to detect the concentration of glucose in solution exhibiting linearity from 0.1 to 10 mM and 50–500 mM with a sensitivity transition from 10 mM to 50 mM. The limit of detection for the determination of glucose was found to be 10 μM. This determination was agreed from both UV–Vis absorption and PL spectroscopy. However, the PL emission method of determination was most suited with its very high accuracy of 98.04 ± 1.96% and 97.33 ± 2.67% for the linear range of glucose concentration within 0.1–10 mM and 50–500 mM, respectively. The PL enhancement was highly selective towards glucose in mixture of other form of sugars making it suitable for determining glucose in food samples.

1. Introduction

Graphene quantum dots (GQD) are the quantum dots derived from graphene or graphene oxide exhibiting the quantum confinement effect in all the three spatial directions [1]. Other sources like monosaccharides and polycyclic molecules, and even multi step organic synthesis using simple organic molecules have also been employed for the synthesis of GQD [2–4]. The finite band gap along with exciton confinement leads to photoluminescence (PL) in GQD. The PL of GQDs is usually observed when the size of quantum dot is reduced under 35 nm [5]. Few noted applications where use of GQDs are explored are photovoltaics [6,7], organic light-emitting diodes [8], fuel cells [9], and most importantly as sensors and biosensors [10,11].

Glucose, owing to its role and importance in dietary supplements and biological system, could be argued to be most important analyte among all. The comprehensive work has already been undertaken in terms of quantitative estimation of glucose in biological assays [12]. Most of these sensors are electrochemical sensors which can be either enzymatic [13,14] or non-enzymatic [15–18]. Electrochemical sensors benefit from very low limit of detection (LOD) intrinsically due to the very high precision which electronics of the signal recorder provides [19]. Therefore, such sensors are often used in determination of analytes in biological systems which accuracy in ppm levels [20]. However, the ultra-low concentration sensitivity means that these sensors are not suitable for detecting glucose in higher concentrations as is the case in food samples. Another limitation of the electrochemical sensors is the complex fabrication of electrodes. Therefore, a PL emission-based sensing approach for glucose can be a looked upon as a complimentary method of analysis. Additionally, such sensors are also reaching ultra-low LOD as low as 16 nM [21]. However, as is the case with electrochemical sensors, the linear range of detection is very low thereby limiting their applications to clinical diagnostics and biomedical applications.

The PL based sensors are usually able to detect glucose in concentration range of 0.1–1000 mM [10]. This range is perfectly suited for testing food samples and other samples where higher concentration of glucose is expected. Syshchyk et al. reported an enzyme biosensor on porous silicon for PL determination of glucose within concentration range of 0–3.0 mM [22]. Yi et al. reported a label free silicon quantum dot PL probe for determining the concentration of glucose in μM range with high specificity [23]. However, the sensing in mM region was not possible using this method. PL carbon dots are looked upon as viable PL sensor for various analytes including glucose [24]. Carbon dots with reduced graphene oxide are shown to be able to detect glucose concentration as low as 140 nM with linear range of determination being 1–60 μM [25]. Qin et al. reported a low cost synthesis of PL carbon dots for determining glucose within linear range of 2–18 mM with LOD being 45

* Corresponding author.
E-mail address: ram@nitk.edu.in (B.R. Bhat).

https://doi.org/10.1016/j.saa.2019.117325
1386-1425/

μM [26]. Zhnag et al. reported B-GQD with linear range of detection being 0.1–10 mM and LOD as 0.03 mM [27]. Another boron rich GQD was reported with same linear range of detection but lower LOD of 5 μM [28]. Few other reports of GQD as PL sensing probe for determination of glucose are available [29,30].

In present report, we discuss the one-pot synthesis and characterization of amine-functionalized GQD (NH_2-GQD) and its applicability for the quantitative detection of glucose. A comprehensive study utilizing both UV–Vis absorbance and PL emission as a tool for the determination of glucose is provided. A stringent error analysis of the determination for both methods is also given. Additionally, commercial samples used to determine the glucose content and a comparative study of reported PL sensor with similar sensor from literature is reported. NH_2-GQD owing to its easy preparation and wide linear range with LOD as low as 0.01 mM makes then suitable to complement already available sensors for diverse applications.

2. Experimental

2.1. Synthesis of NH_2-GQD

The amine functionalized GQDs were synthesized using Graphene oxide (GO) obtained from improved Hummer's method [31]. The preparation of NH_2-GQD was carried out using hydrothermal method [32] with modifications. In a typical procedure, the as-prepared GO dispersed in water was brought to pH 10 using NaOH. Further, 18 ml of this mixture with 2 ml hexamethylenetetramine (HMTA) was taken in an autoclave with Teflon lining and heated at 200 °C for 12 h. The resultant dispersion was then filtered followed by dialysis in a dialysis bag (retained molecular weight: 3500 Da) overnight to yield strongly fluorescent quantum dots. The concertation NH_2-GQD obtained was ~1 mg/ml. The PL was observed in UV Cabinet with the irradiation of 365 nm which was indicative of the synthesis of quantum dots. Same method was followed without the addition of HMTA to synthesize GQD.

2.2. Material characterization

The FTIR spectra of the quantum dots were obtained on BRUKER FTIR spectrometer with Eco-ATR accessory. Raman spectra of the samples were obtained using a Renishaw Raman microscope using 514 nm laser excitation at room temperature. Quantum dots were examined under the transmission electron microscope (JEM-2100 Plus Transmission Electron Microscope) for their morphology and size determination. UV–Vis spectra were recorded on Analytik Jena Specord S600 UV–Vis spectrophotometer. All the PL measurements were made on Horiba Fluoromax Spectrofluorometer.

2.3. Determination of glucose

The determination of glucose was carried out using standard solutions of glucose with varying concentrations (from 0.1 mM to 500 mM) for obtaining calibration curve. The concentration of NH_2-GQD used was 1 mg/ml with glycine sodium hydroxide buffer to maintain pH 10 during the estimation. Few test solutions of glucose were prepared to check the error in determination. The commercial glucose instant mix was dissolved in distilled water in predetermined amount. The resulting solutions were filtered through 47 μm membrane filter to undissolved and other colloidal matter followed by further dilution to check the suitability of method for real samples.

The % error in determination was calculated using formula:

$$\%\text{Error} = \frac{(\text{Observed Value} - \text{Actual Value}) \times 100}{\text{Actual Value}}$$

The relative UV–Vis absorbance of for the monosaccharide and disaccharide interacted NH2-GQD was calculated using formula:

$$\text{Relative Absorbance} = \frac{\text{Absorbance of Sample (A)} - \text{Absorbance of Blank (A}_o\text{)}}{\text{Absorbance of Glucose (A}_g\text{)} \backslash - \text{Absorbance of Blank (A}_o\text{)}}$$

The relative PL emission of for the monosaccharide and disaccharide interacted NH2-GQD was calculated using formula:

$$\text{Relative PL Emission} = \frac{\text{PL emission of Sample (I)} - \text{PL emission of Blank (I}_o\text{)}}{\text{PL emission of Glucose (I}_g\text{)} - \text{PL emission of Blank (I}_o\text{)}}$$

3. Results and discussion

3.1. Characterization of GQD and NH_2-GQD

The distinction between GQD and NH_2-GQD was ascertained using FTIR spectroscopy (Fig. 1a). FTIR spectrum of GQD was observed with characteristic peaks at 3500 cm^{-1} (broad) and 1700 cm^{-1} (sharp) corresponding to —OH stretching and —C═O stretching, respectively. In the spectrum of NH_2-GQD, the presence of additional side peak at

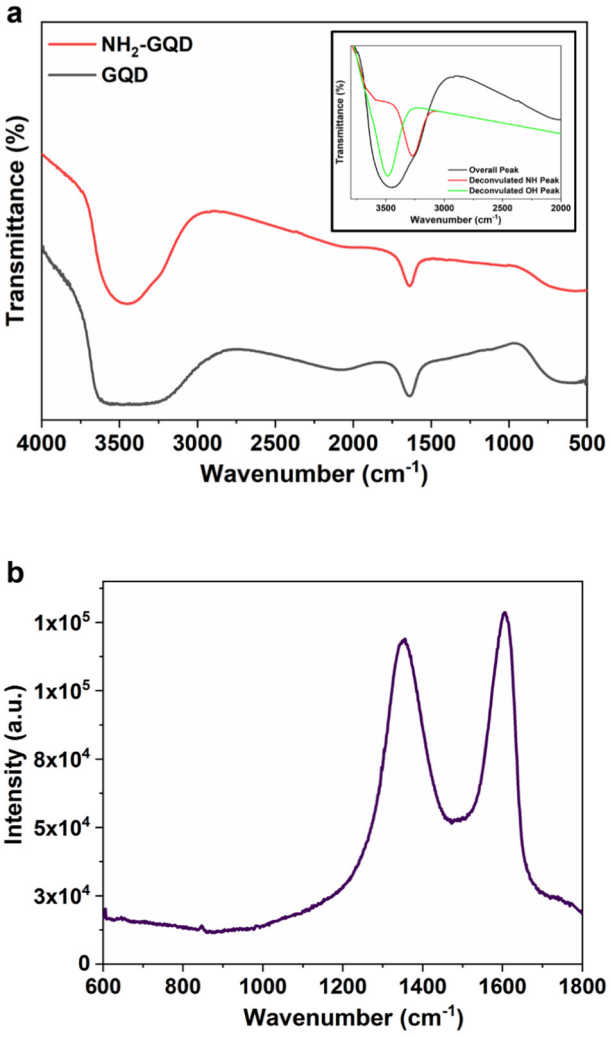

Fig. 1. a) FTIR spectra of GQD and NH_2-GQD with deconvoluted peak of N—H and O—H stretching in NH_2-GQD (inset); b) Raman spectra of NH_2-GQD.

3300 cm^{-1} due to NH stretching along with 3500 cm^{-1} for OH stretching is clear evidence for the amine functionalization of GQD (Inset Fig. 1a). There was a slight shift in —C═O stretching peak to 1680 cm^{-1} in spectrum of NH_2-GQD indicated the presence of amide groups on NH_2-GQD as well. The Raman spectrum of NH_2-GQD was recorded to assess the nature of edges (Fig. 1b). NH_2-GQD showed characteristic D band and G band associated with at1350 cm^{-1} and 1580 cm^{-1}, respectively. The disordered C atoms at the edges of NH_2-GQD generate D band in the Raman spectrum, whereas the G band is result of to the in-plane vibration of sp^2-bonded C atoms. There is an appreciable loss of graphitic layered structure as evident from 1:1 ratio of D and G band intensities. Conventionally, the intensity ratio hints towards the formation of single to few atomic layer (bi- or tri-) thick NH_2-GQD. However, the D band in NH_2-GQD is of higher intensity than in graphene as the fraction of carbon atoms present of edge with respect to those in the core is higher than the graphene. Therefore, intensity ratio is not the ideal indicator of the number of layers in the quantum dot. Kim et al. reported similar understanding about the Raman spectra of GQD [33]. This can be emphasized by TEM of NH_2-GQD, where the NH_2-GQD appears darker than expected which means that there are more than bi- or tri- atomic layers thick (Fig. 3a).

The bonding in NH_2-GQD was further determined by XPS analysis (Fig. 2). The survey scan of NH_2-GQD was observed with peaks at 284 eV, 400 eV, and 532 eV corresponding to C, N, and O atoms, respectively (Fig. 2a). The low intensity of N peak suggests that fraction of N atom in quantum dot is low as compared to C and O which is the usual case with GQD. C and O atoms form core of the GQD whereas the functionalization with N just happen over few sites on the edge of the GQD and possibly as dopant in the GQD core. Hence in NH_2-GQD, the overall fraction of N will always be less than that of C and O which is supported by the survey scan. The C specific XPS scan and deconvoluted peaks are given in Fig. 2b. The peaks at 284 eV, 286 eV, and 288 eV are due to C—C, C—O—C, and C═O carbons of NH_2-GQD. The C available for C—C bonds being maximum leads to a highly intense peak followed by low intensity peak due to C═O. The GQDs are cut along C—O—C bonds present in graphene oxide, therefore, very few such bonds are left in NH_2-GQD hence a very low intensity peak. The N specific scan in given in Fig. 2c. The presence of N is ascertained by observing peak at 398 eV. This indicates that few C atoms in the GQD cores were replaced to N atom, resulting in N-doping of GQD. Further, the N atoms occupying C—NH_2 bonds at the edges of GQD were observed at 400 eV. The O specific scan of NH_2-GQD reaffirmed the presence of C—O and C═O bonds in the quantum dots by reflecting peaks at 529 eV and 532 eV, respectively. The XPS analysis made the presence of the three primary atoms, C, N, and O evident in the NH_2-GQD sample along with the bond there are present in. Among all the bonds which were consistent with the FTIR spectra, presence of XPS peak corresponding to N at 398 eV, which can be attributed to the N occupying few positions in the all carbon skeleton of GQD lead to the conclusive evidence of N doping in the GQD via reported method. Table 1 presents the calculated percentage of element and bond present in the GQD. It should be noted that the edges of GQD are highly passivated with oxygen bearing functional group, few of which undergo amination of result in NH_2-GQD. Therefore, it is not surprising to see higher percentage of oxygen and oxygen rich functional groups in the table.

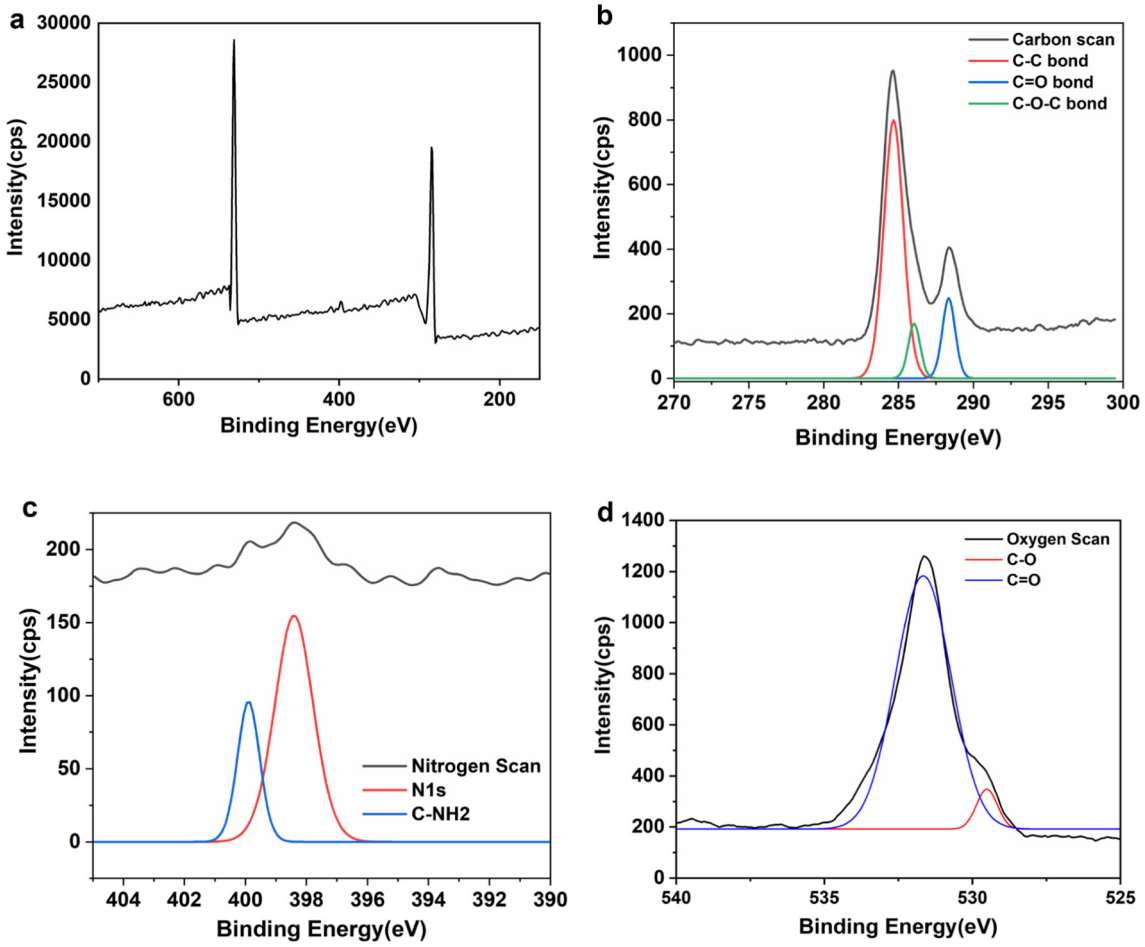

Fig. 2. a) XPS Survey scan of NH_2-GQD; b) XPS C specific scan of NH_2-GQD; c) XPS N specific scan of NH_2-GQD; and d) XPS O specific scan of NH_2-GQD.

Table 1
Composition of NH_2-GQD as calculated from XPS.

S. no.	Element	Binding energy (eV)	Peak area	Elemental %
1	Carbon	284.8	1503.13	41.18
2	Nitrogen	398	249.53	6.84
3	Oxygen	533	1897.63	51.99
S. no.	Bond	Binding energy (eV)	Peak area	Bond %
1	C—C	284.8	1322.10	30.38
2	O—C═O	288.5	273.99	6.30
3	C—O—C	286.0	172. 90	3.97
4	C—NH_2	400.0	105.10	2.41
5	C—OH	531.6	139.59	3.21
6	C═O	533	2338.55	53.73

The transmission electron micrograph of NH_2-GQD was recorder to analyze apparent thickness and size distribution of the quantum dots (Fig. 3a). The NH_2-GQD were of various atomic thickness which coupled with Raman analysis (as given in Fig. 1b) led to the conclusion to be of few atomic layers thick. The average particle size encountered for these quantum dots was 5 nm with 90% quantum dots being within 3–10 nm. The interaction of NH_2-GQD with glucose lead to aggregation of the quantum dots which can be visualized in Fig. 3b. The average particle size increased to 8 nm with 90% of the quantum dots being within 5–12 nm. Therefore, the NH_2-GQD bond to glucose molecule which leads to the larger size quantum dots. The size of the aggregated quantum dots is approximately double that of the as synthesized NH_2-GQD. This apparent doubling of the aggregate size leads to the conclusion that stochiometric ration of NH_2-GQD to glucose in the aggregated quantum dots is 2:1. The possible mode of interaction between the NH_2-GQD and glucose in given in Scheme 1. The apparent effect of this aggregation of quantum dots over the UV–vis absorption and PL emission is further studied by recording respective spectra.

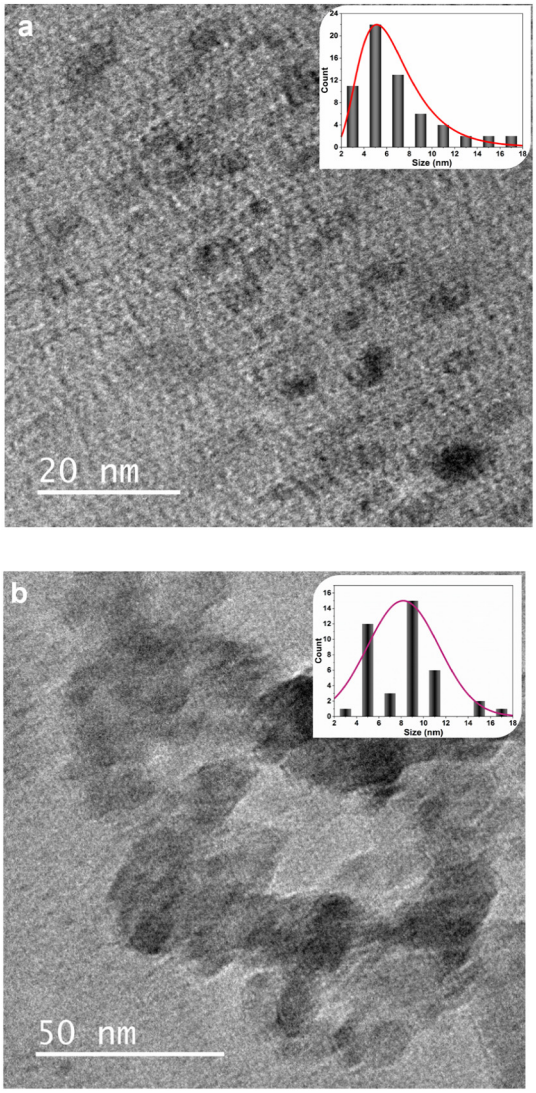

Fig. 3. a) Transmission electron micrograph of NH_2-GQD with size distribution (Inset); b) Transmission electron micrograph of NH_2-GQD aggregated along glucose with size distribution (Inset).

The UV–vis absorption and PL spectra of NH_2-GQD are given in Fig. 4. The UV–vis spectrum of NH_2-GQD showed that the onset of the absorption for the quantum dots is at ~380 nm. Therefore, the bandgap of NH_2-GQD is 3.26 eV. The maximum absorbance is observed at 260 nm (λ_{max}). This wavelength was used to study the UV–Vis absorbance-based sensing pattern of NH_2-GQD for glucose. The PL spectra of NH_2-GQD was recorded by exciting the quantum dot by an incident electromagnetic beam of wavelength 380 nm. This wavelength was chosen to observe the visible PL as any shorter wave leads to PL in shorter wave regions which is difficult to observe visually. The PL of the NH_2-GQD if set in visible region leads makes the observation of visual alteration in intensity possible. Hence, this can make qualitative determination of analytes possible. The highest intensity of the PL was observed at 480 mm for NH_2-GQD. Therefore, the intensity of PL was recorded at 480 nm was used to study the PL-based sensing pattern of NH_2-GQD for glucose.

3.2. Mechanism of aggregation induced photoluminescence emission in glucose-NH_2-GQD system

The mode of interaction between glucose and NH_2-GQD is given in Scheme 1. The approximate 2-fold increase in the size of quantum dot aggregate w.r.t the size of NH2-GQD hint towards the 2:1 stochiometric ratio of NH_2-GQD to glucose in the highly luminescence quantum dot aggregate, wherein two NH_2-GQD are linked by a glucose linker. The chemical structure drawn in the schematic is for representation purpose to depict the position of active amine groups which plausibly binds to the hydroxyl groups of glucose. NH_2-GQD does not have a well-defined chemical formula as it is more of a functional material than a molecule. The apparent increase in the intensity of PL emission of NH_2-GQD when interacted with glucose is also due to the NH_2-GQD glucose aggregates. Zhang et al. earlier reported that cis-5,6-diol units of glucose binds to two functionalized GQD [27]. The intramolecular rotation of the luminescence center in the aggregates involves simultaneous movements of the glucose linker and another neighboring luminescence center. The high energy barrier of such motions rigids the aggregate thereby blocking the nonradiative relaxation channels, and populating the radiative decay, in turn making the luminescence center highly emissive [34–36]. Additionally, the PL emission of the NH_2-GQD is highest in pH 10 which was made stable by the addition of glycine-sodium hydroxide buffer (0.08 M). The glucose-NH_2-GQD aggregate also returned highest emission in pH 10.

3.3. UV–vis absorbance method and PL emission method on determination of glucose

The variation of the intensity of absorbance with respect to the concentration of glucose ($C_{glucose}$) is given in Fig. 5a. The marginal ncrease in the absorption was observed when the $C_{glucose}$ was increased. The maximum absorption for the glucose NH_2-GQD system was found to be at 260 nm. All the absorption intensities of various glucose NH_2-

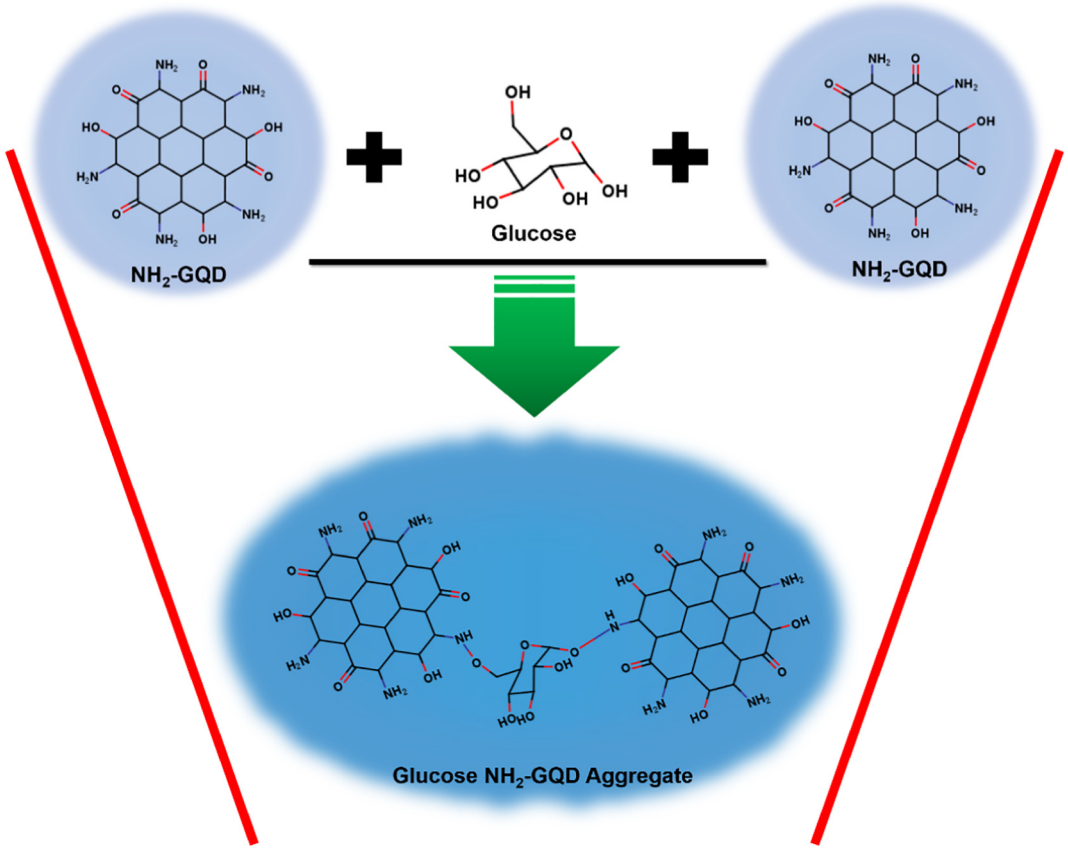

Scheme 1. The plausible mode of interaction between NH_2-GQD and glucose in 2:1 stochiometric ration in aggregated quantum dot.

GQD system were recorded at 260 nm. There was a relatively sharp increase in the intensity as the $C_{glucose}$ is increased from 0.1 mM to 10 mM as compared to 50 mM to 500 mM. The transition in sensitivity was observed for $C_{glucose}$ within 10 mM to 50 mM (Fig. 5b). The stark difference in sensitivities is evident from the difference in slopes of the calibration curve. The calibration curve for the $C_{glucose}$ from 0.1 mM to 10 mM determined with slope of 0.014 with R-square value of 0.9909 and most of the points being in the 95% confidence band of the linear trend (Fig. 5c). Compared to this, the calibration curve for the $C_{glucose}$ from 50 mM to 500 mM determined with slope of 0.00026 with R-square value of 0.99305, again most of the points being in the 95% confidence band of the linear trend (Fig. 5d). The apparent increase in the absorbance intensity is higher for $C_{glucose}$ within 0.1 mM to 10 mM hence is much more suitable range for the determination of glucose. However, the absolute range of the variation of absorption intensity is ~0.3 a.u is low. Therefore, this may induce a larger error in the measurement of $C_{glucose}$ in real sample and also hamper the sensitivity. To overcome these limitations, the PL of the NH_2-GQD was considered to be a viable alternative. NH_2-GQD showed absorbance at 260, 280, 325 and 380 nm. The absorbance of 380 nm radiation leads to visible PL at 480 nm in the NH_2-GQD as observed in Fig. 4. The 380 nm absorbance was also found to be increasing with the increase in the $C_{glucose}$, therefore the PL intensity was also presumed to in increasing. The selection of the excitation wavelength of 380 nm while recording the emission spectra within the range of 430 to 650 nm was to eliminate the PL of water that is observed at 430 nm when excited with a wavelength of 350 nm.

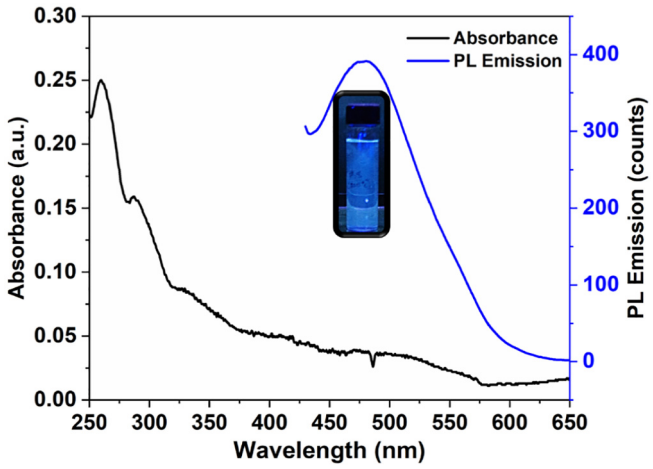

Fig. 4. UV–Vis and Photoluminescence spectra of NH2-GQD recorded within 250–650 nm and 420–650 nm, respectively. The Photoluminescence spectrum was recorded for incident electromagnetic wave of wavelength 380 nm.

The variation of the intensity of PL emission spectra recorded at the excitation wavelength of 380 nm with respect to the $C_{glucose}$ is given in Fig. 6a. The increase in the PL emission was observed when the $C_{glucose}$ was increased. The variation in the intensity of absorbance spectra, the increase in the PL emission is observably more prominent due to the earlier described aggregation induced emission. The maximum PL emission for the glucose NH_2-GQD system was found to be at 480 nm. Therefore, all the absorption intensities for various glucose NH_2-GQD system were recorded at 480 nm. Again, as observed in the case of UV–Vis absorption spectra, there was a relatively sharp increase in the PL emission intensity as the $C_{glucose}$ was increased from 0.1 mM to 10 mM as compared to 50 mM to 500 mM. The transition in sensitivity

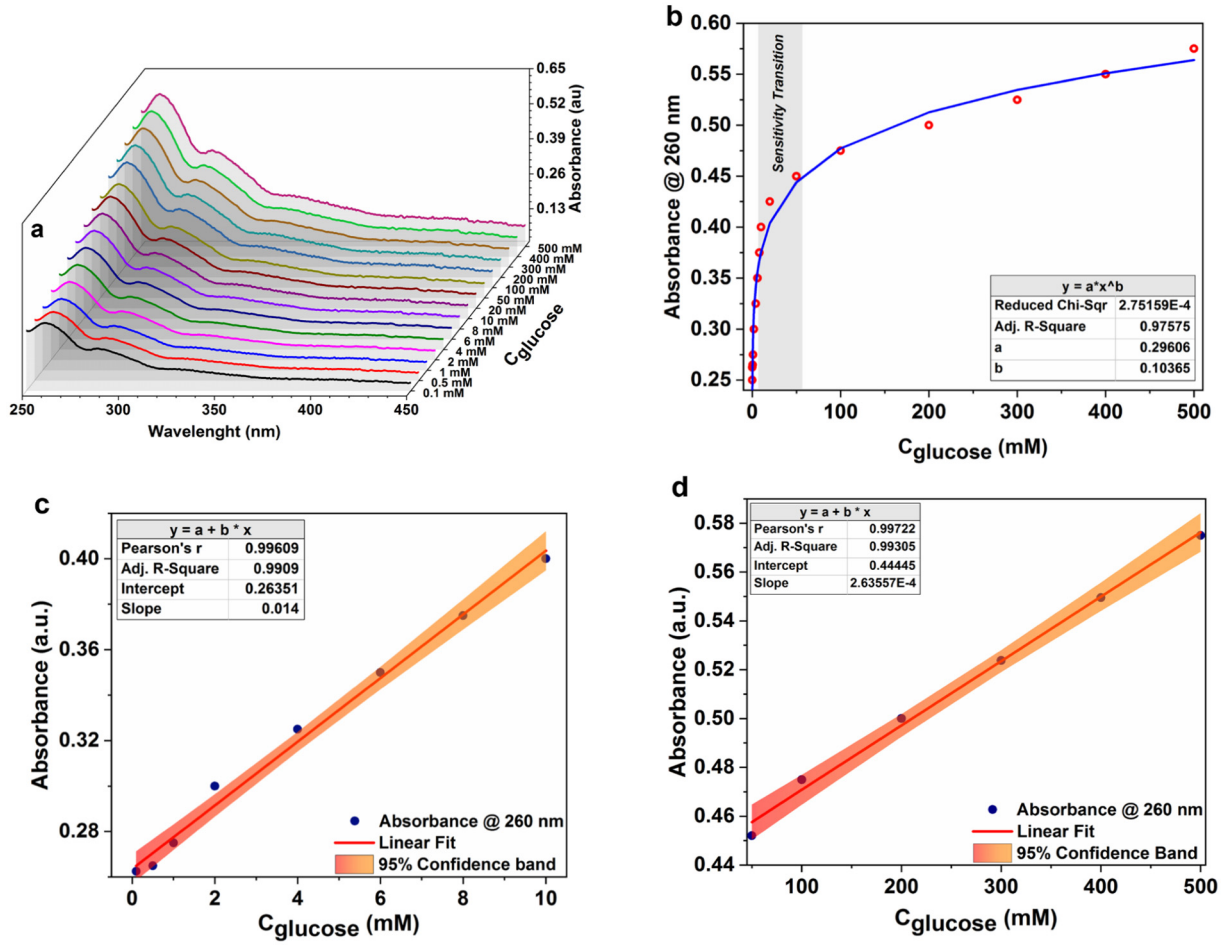

Fig. 5. a) The variation on the UV–Vis absorbance spectra of 1 mM NH_2-GQD at varying concentrations of glucose (0.1 mM to 500 mM); b) variation of UV–Vis absorbance at 260 nm for varying concentrations of glucose (0.1 mM to 500 mM) with non-linear fit data; c) variation of UV–Vis absorbance at 260 nm for varying concentrations of glucose (0.1 mM to 10 mM) with linear fit data and 95% confidence band; d) variation of UV–Vis absorbance at 260 nm for varying concentrations of glucose (50 mM to 500 mM) with linear fit data and 95% confidence band.

was again observed for $C_{glucose}$ within 10 mM to 50 mM (Fig. 6b). The pronounced difference in sensitivities is evident from the difference in slopes of the calibration curve. The calibration curve for the $C_{glucose}$ from 0.1 mM to 10 mM was determined with slope of 21.80384 with R-square value of 0.99139 and most of the points being in the 95% confidence band of the linear trend (Fig. 6c). Compared to this, the calibration curve for the $C_{glucose}$ from 50 mM to 500 mM determined with slope of 0.60315 with R-square value of 0.98971, again with most of the points being in the 95% confidence band of the linear trend (Fig. 6d). The apparent increase in the PL intensity is higher for $C_{glucose}$ within 0.1 mM to 10 mM hence is much more suitable range for the determination of glucose. Unlike the UV–Vis absorbance spectra, the absolute range of the variation of PL intensity is ~650 counts which is significantly higher. Therefore, this reduces the error in the measurement of $C_{glucose}$ in real sample and also improves the sensitivity.

3.4. Errors and accuracy of determination of glucose

The errors observed in the determination of $C_{glucose}$ by both UV–Vis absorbance and PL emission methods along for the concentration range 0.1 to 10 mM and 50 to 500 mM is given as Fig. 7. As expected, the lower range of absolute variation within the least and highest UV–Vis absorbance observed for the glucose NH_2-GQD system within lowest and highest $C_{glucose}$, showed larger error in measurement as compared to the measurement done by recording the PL emission (Fig. 7 and b). The slope for the variation of UV–Vis absorbance and PL emission was higher for the $C_{glucose}$ varying from 0.1 mM to 10 mM than that of $C_{glucose}$ varying from 50 mM to 500 mM, respectively. Therefore, the overall error in measurement was lower in the test samples which were within concertation 0.1 mM to 10 mM (Fig. 7c). The average % error for the absorbance method of determination of glucose were obtained as 6.60% and 9.87% for the $C_{glucose}$ range of 0.1–10 mM and 50–500 mM, respectively. Therefore, the method returned an accuracy of 93.4 ± 6.60% and 90.13 ± 9.87% for $C_{glucose}$ range of 0.1–10 mM and 50–500 mM, respectively. For the emission method of determination, the average % error obtained for same determination was 1.96% and 2.67% for the $C_{glucose}$ range of 0.1–10 mM and 50–500 mM, respectively. Hence the accuracy of PL emission method of sensing for $C_{glucose}$ range of 0.1–10 mM and 50–500 mM are 98.04 ± 1.96% and 97.33 ± 2.67%, respectively. Therefore, the emission method for the quantitative analysis of glucose is more accurate in both the concentration regions. Additionally, careful selection of the concentration range suitable for linearity in PL emission makes determination of glucose of very wide concentration variance possible.

3.5. Selectivity of sensing methods

Fig. 8 presents the relative absorbance and relative PL intensity of various sugars (Fructose, Galactose, mannose, Sucrose, Lactose and

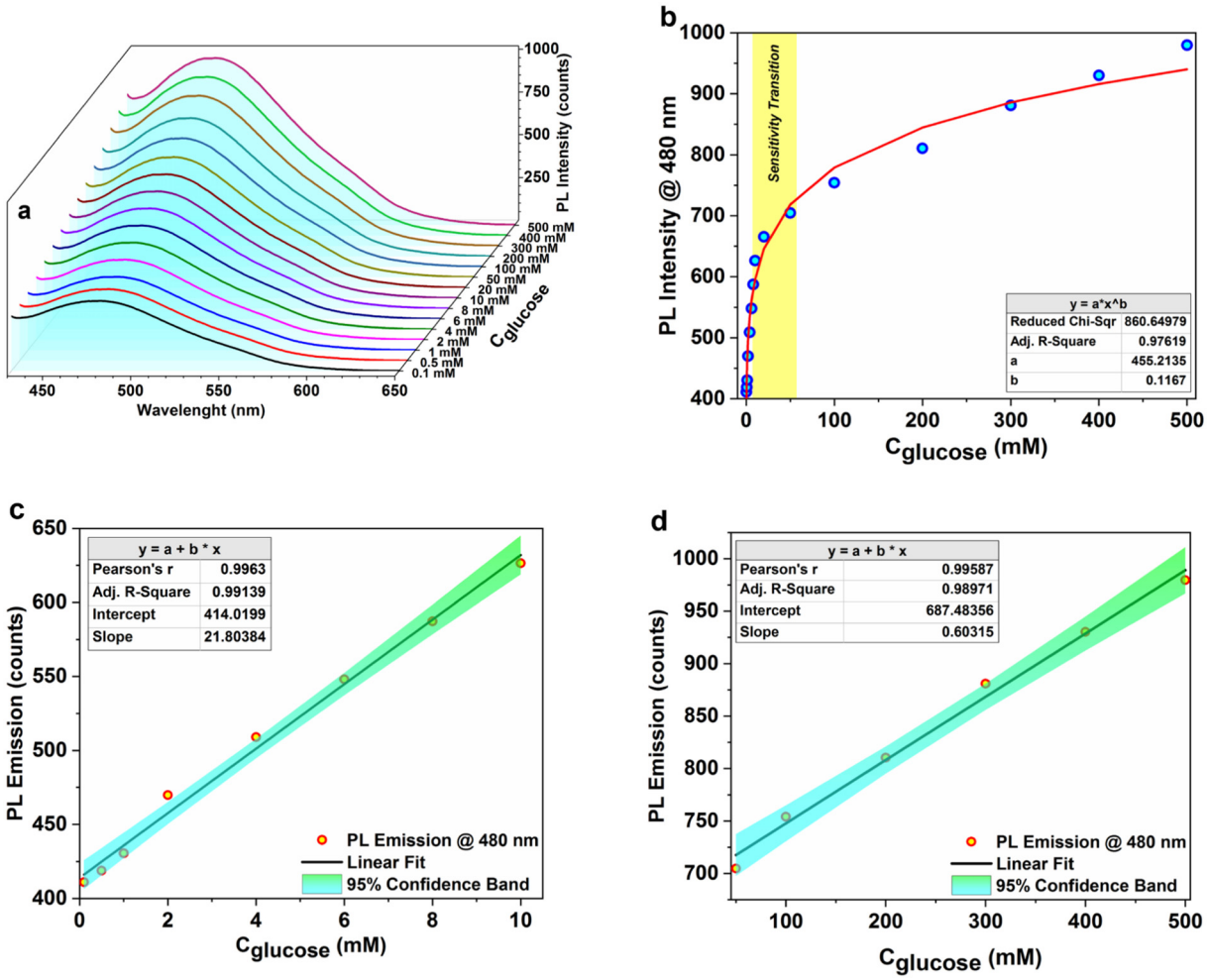

Fig. 6. a) The variation on the photoluminescence spectra of 1 mM NH_2-GQD at varying concentrations of glucose (0.1 mM to 500 mM); b) variation of photoluminescence intensity at 480 nm for varying concentrations of glucose (0.1 mM to 500 mM) with non-linear fit data; c) variation of photoluminescence intensity at 480 nm for varying concentrations of glucose (0.1 mM to 10 mM) with linear fit data and 95% confidence band; d) variation of photoluminescence intensity at 480 nm for varying concentrations of glucose (50 mM to 500 mM) with linear fit data and 95% confidence band.

Maltose) in comparison to glucose at 10 mM concentration. The earlier comments made about the sensitivity of the probe for determination of the glucose in real samples can be again strengthen by the comparison of selectivity of the UV–Vis absorbance and PL emission-based determination of glucose in the sample in presence of other types of sugar. The relative absorbance of the glucose when compared to other sugars shows that the NH_2-GQD is slightly selectivity towards glucose (Fig. 8a). The monosaccharides exhibit significant relative absorbance when compared to glucose as opposed to disaccharides. However, the relative PL intensity for glucose is significantly higher compared to both monosaccharides and disaccharides (Fig. 8b), which display highly selectivity nature of NH_2-GQD as a PL sensory probe for the determination of glucose.

3.6. Determination of glucose in real samples

The determination of glucose in real samples was performed using commercial Glucon D, Glucon D lime, and Glucon D orange, all manufactured by Kraft Heinze India. As per the nutritional fact, the glucose content in Glucon D, Glucon D lime, and Glucon D orange are 91%, 47% and 36% w/w, respectively. The PL emission method was employed for the determination for all the samples. The samples were dissolved in distilled water to obtain sample concertation of 8 mM. The % composition of glucose by emission method for Glucon D, Glucon D lime, and Glucon D orange were obtained as 90.24%, 45.98% and 37.02% w/w, respectively. These determinations are within ~ accuracy of 98 ± 2% %, which agrees with the earlier mentioned error analysis.

The reported methods were compared with earlier reported literatures pertaining to the detection of glucose via photoluminescence emission method with various functionalized GQDs. The reported PL emission method of determining glucose was found to be superior in terms of the wide detection range of 0.1 mM to 500 mM (with transition in sensitivity between 10 and 50 mM) with high accuracy of 98.04 ± 1.96% and 97.33 ± 2.67% for linear range of 0.1–10 mM and 50–500 mM, respectively. The determination of accuracy for the PL sensing ability of functionalized GQD is also presented for the first time to the best of author's information. Table 2 summarize the comparison of detection of glucose using few carbon dots or functionalized GQD reported in literature with the presented study.

4. Conclusions

The amine functionalized graphene quantum dots were prepared in a one pot hydrothermal method using graphene oxide and hexamethylenetetramine. The obtained quantum dots exhibited all

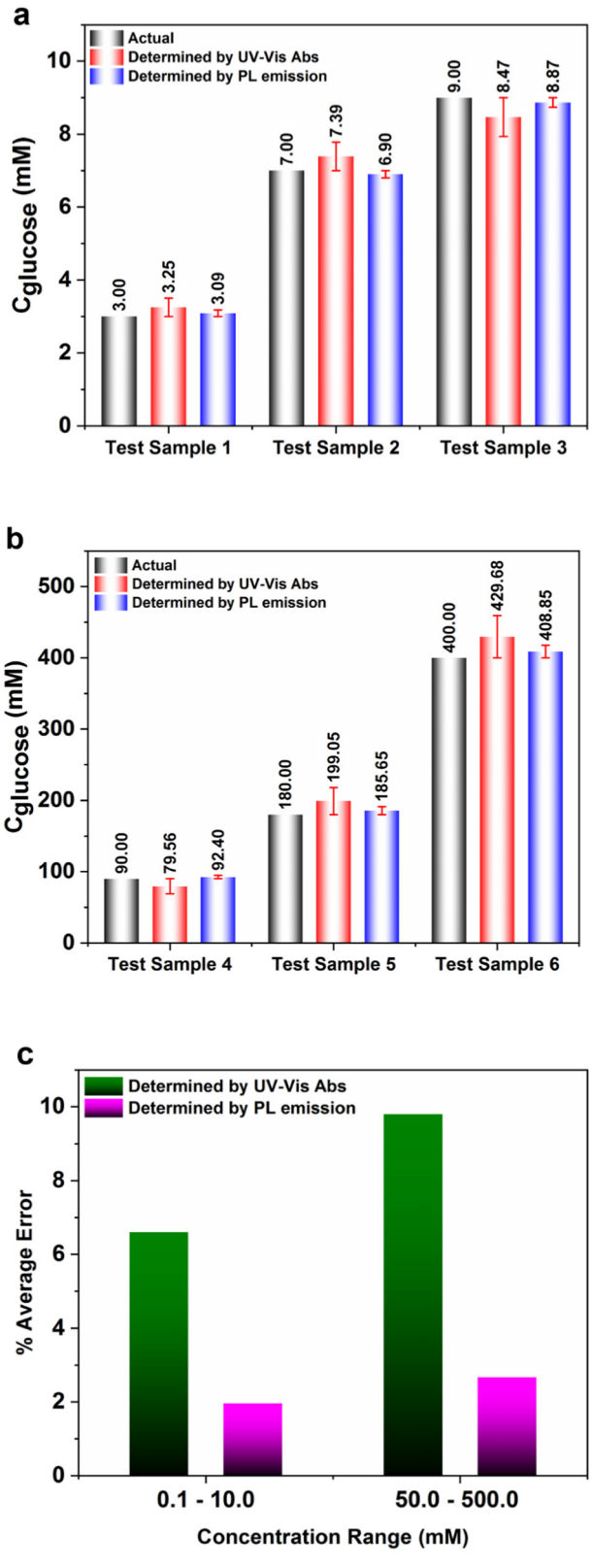

Fig. 7. a) Determination of $C_{glucose}$ in test sample 1 (3 mM), test sample 2 (7 mM) and test sample 3 (9 mM) using UV–Vis absorption calibration curve and PL intensity calibration curve with absolute errors; b) Determination of $C_{glucose}$ in test sample 4 (90 mM), test sample 5 (180 mM), and test sample 6 (400 mM) using UV–Vis absorption calibration curve and PL intensity calibration curve with absolute errors; c) % Average Error for determination of $C_{glucose}$ using UV–Vis absorption calibration curve and PL intensity calibration curve within the range of 0.1–10 mM and 50–500 mM.

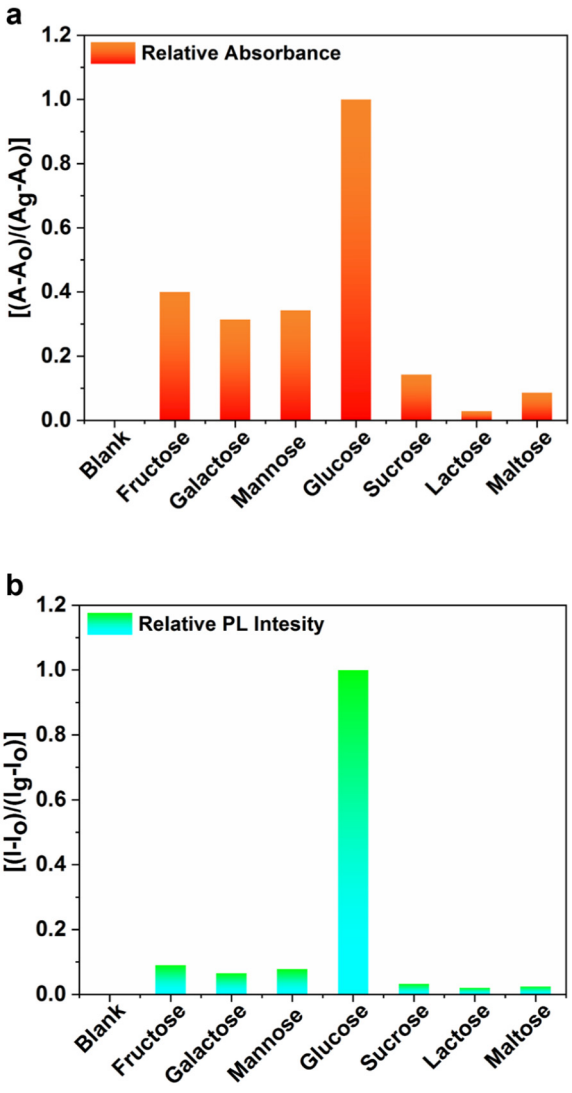

Fig. 8. a) Relative absorbance of glucose in comparison to various sugars (Fructose, Galactose, mannose, Sucrose, Lactose and Maltose) with all sugar solutions with concentration of 10 mM; b) Relative photoluminescence intensity of glucose in comparison to various sugars (Fructose, Galactose, mannose, Sucrose, Lactose and Maltose) with all sugar solutions with concentration of 10 mM.

the predicted characteristics in the series of characterizations including FTIR, Raman, XPS, and TEM analysis. The enhancement of PL emission in the NH_2-GQD in presence of glucose was due to the aggregate formation of which was well supported by the TEM analysis. This resulted in the significantly larger increase in PL intensity on addition of glucose in varying amounts. The UV–Vis absorbance and PL emission methods were evaluated for the determination of glucose. The PL emission method was significantly better with dual linear range 0.1–10 mM and 50–500 mM with an accuracy of 98.04 ± 1.96% and 97.33 ± 2.67%, respectively. The LOD for the PL emission method was obtained to be 0.01 mM. The analysis of commercially available glucose instant mixes was analyzed, and the results were obtained with ~98 ± 2% accuracy. Therefore, the NH_2-GQD was deemed to be a suited photoluminescent probe for the detection of glucose.

Declaration of Competing Interest

There are no conflicts of interest to declare.

Table 2
Graphene quantum dots for PL detection of glucose.

S. no.	Type of GQD	Precursor	Linear range (mM)	LOD (mM)	Error (%)	Sample	Ref
1	Carbon dot	Willow bark	2–18	0.045	NM	Human blood serum	[26]
2	BBV–GQD	Graphene	1–60	NM	NM	Aqueous solution	[29]
3	B-GQD	Boron doped graphene	0.1–10	0.03	NM	NM	[27]
4	APBA-GQD	Graphene oxide	0.1–10	0.005	NM	Rat brain microdialysate	[28]
5	GQD	Glucose	5–50	NM	NM	NM	[30]
6	NH_2-GQD	Graphene oxide	0.1–10	0.01	1.96	Commercial glucose mix	This work
			50–500		2.67		

Acknowledgment

The author, Mr. Praveen Mishra would like to acknowledge National Institute of Technology Karnataka for extending the research fellowship.

References

[1] M. Bacon, S.J. Bradley, T. Nann, Graphene quantum dots, Part. Part. Syst. Charact. 31 (2014) 415–428.
[2] L. Tang, R. Ji, X. Li, K.S. Teng, S.P. Lau, Size-dependent structural and optical characteristics of glucose-derived graphene quantum dots, Part. Part. Syst. Charact. 30 (2013) 523–531.
[3] R. Liu, D. Wu, X. Feng, K. Müllen, Bottom-up fabrication of photoluminescent graphene quantum dots with uniform morphology, J. Am. Chem. Soc. 133 (2011) 15221–15223.
[4] X. Yan, X. Cui, L.-s. Li, Synthesis of large, stable colloidal graphene quantum dots with tunable size, J. Am. Chem. Soc. 132 (2010) 5944–5945.
[5] S. Kim, S.W. Hwang, M.-K. Kim, D.Y. Shin, D.H. Shin, C.O. Kim, S.B. Yang, J.H. Park, E. Hwang, S.-H. Choi, G. Ko, S. Sim, C. Sone, H.J. Choi, S. Bae, B.H. Hong, Anomalous behaviors of visible luminescence from graphene quantum dots: interplay between size and shape, ACS Nano 6 (2012) 8203–8208.
[6] I.P. Hamilton, B. Li, X. Yan, L.-s. Li, Alignment of colloidal graphene quantum dots on polar surfaces, Nano Lett. 11 (2011) 1524–1529.
[7] V. Gupta, N. Chaudhary, R. Srivastava, G.D. Sharma, R. Bhardwaj, S. Chand, Luminscent graphene quantum dots for organic photovoltaic devices, J. Am. Chem. Soc. 133 (2011) 9960–9963.
[8] L. Tang, R. Ji, X. Cao, J. Lin, H. Jiang, X. Li, K.S. Teng, C.M. Luk, S. Zeng, J. Hao, S.P. Lau, Deep ultraviolet photoluminescence of water-soluble self-passivated graphene quantum dots, ACS Nano 6 (2012) 5102–5110.
[9] Y. Li, Y. Zhao, H. Cheng, Y. Hu, G. Shi, L. Dai, L. Qu, Nitrogen-doped graphene quantum dots with oxygen-rich functional groups, J. Am. Chem. Soc. 134 (2012) 15–18.
[10] S. Benítez-Martínez, M. Valcárcel, Graphene quantum dots in analytical science, TrAC Trends Anal. Chem. 72 (2015) 93–113.
[11] R. Xie, Z. Wang, W. Zhou, Y. Liu, L. Fan, Y. Li, X. Li, Graphene quantum dots as smart probes for biosensing, Anal. Methods 8 (2016) 4001–4016.
[12] N.S. Oliver, C. Toumazou, A.E.G. Cass, D.G. Johnston, Glucose sensors: a review of current and emerging technology, Diabet. Med. 26 (2009) 197–210.
[13] I. Lee, N. Loew, W. Tsugawa, K. Ikebukuro, K. Sode, Development of a third-generation glucose sensor based on the open circuit potential for continuous glucose monitoring, Biosens. Bioelectron. 124–125 (2019) 216–223.
[14] K.B. Kim, W.-C. Lee, C.-H. Cho, D.-S. Park, S.J. Cho, Y.-B. Shim, Continuous glucose monitoring using a microneedle array sensor coupled with a wireless signal transmitter, Sensors Actuators B Chem. 281 (2019) 14–21.
[15] Y. Li, M. Xie, X. Zhang, Q. Liu, D. Lin, C. Xu, F. Xie, X. Sun, Co-MOF nanosheet array: a high-performance electrochemical sensor for non-enzymatic glucose detection, Sensors Actuators B Chem. 278 (2019) 126–132.
[16] Y. Du, Y. He, Z. Zheng, X. Shen, Y. Zhou, T. Wang, Z. Zhu, C. Wang, A renewable platform for high-performance glucose sensor based on co(OH)2 nanoparticles/three-dimensional graphene frameworks, J. Electrochem. Soc. 166 (2019) B42–B48.
[17] A. Diouf, B. Bouchikhi, N. El Bari, A nonenzymatic electrochemical glucose sensor based on molecularly imprinted polymer and its application in measuring saliva glucose, Mater. Sci. Eng. C 98 (2019) 1196–1209.
[18] L. Wang, C. Peng, H. Yang, L. Miao, L. Xu, L. Wang, Y.J.J.o.M.S. Song, Ni@carbon nanocomposites/macroporous carbon for glucose sensor, J. Mater. Sci., 54 (2019) 1654-1664.
[19] J. Wang, Electrochemical Glucose Biosensors, Chem. Rev. 108 (2008) 814–825.
[20] C. Chen, Q. Xie, D. Yang, H. Xiao, Y. Fu, Y. Tan, S. Yao, Recent advances in electrochemical glucose biosensors: a review, RSC Adv. 3 (2013) 4473–4491.
[21] Y.-L.T. Ngo, W.M. Choi, J.S. Chung, S.H. Hur, Highly biocompatible phenylboronic acid-functionalized graphitic carbon nitride quantum dots for the selective glucose sensor, Sensors Actuators B Chem. 282 (2019) 36–44.
[22] O. Syshchyk, V.A. Skryshevsky, O.O. Soldatkin, A.P. Soldatkin, Enzyme biosensor systems based on porous silicon photoluminescence for detection of glucose, urea and heavy metals, Biosens. Bioelectron. 66 (2015) 89–94.
[23] Y. Yi, J. Deng, Y. Zhang, H. Li, S. Yao, Label-free Si quantum dots as photoluminescence probes for glucose detection, Chem. Commun. 49 (2013) 612–614.
[24] P. Roy, P.-C. Chen, A.P. Periasamy, Y.-N. Chen, H.-T. Chang, Photoluminescent carbon nanodots: synthesis, physicochemical properties and analytical applications, Mater. Today 18 (2015) 447–458.
[25] T.-Y. Yeh, C.-I. Wang, H.-T. Chang, Photoluminescent C-dots@RGO for sensitive detection of hydrogen peroxide and glucose, Talanta 115 (2013) 718–723.
[26] X. Qin, W. Lu, A.M. Asiri, A.O. Al-Youbi, X. Sun, Green, low-cost synthesis of photoluminescent carbon dots by hydrothermal treatment of willow bark and their application as an effective photocatalyst for fabricating Au nanoparticles–reduced graphene oxide nanocomposites for glucose detection, Cat. Sci. Technol. 3 (2013) 1027–1035.
[27] L. Zhang, Z.-Y. Zhang, R.-P. Liang, Y.-H. Li, J.-D. Qiu, Boron-doped graphene quantum dots for selective glucose sensing based on the "abnormal" aggregation-induced photoluminescence enhancement, Anal. Chem. 86 (2014) 4423–4430.
[28] Z.-b. Qu, X. Zhou, L. Gu, R. Lan, D. Sun, D. Yu, G. Shi, Boronic acid functionalized graphene quantum dots as a fluorescent probe for selective and sensitive glucose determination in microdialysate, Chem. Commun. 49 (2013) 9830–9832.
[29] Y.-H. Li, L. Zhang, J. Huang, R.-P. Liang, J.-D. Qiu, Fluorescent graphene quantum dots with a boronic acid appended bipyridinium salt to sense monosaccharides in aqueous solution, Chem. Commun. 49 (2013) 5180–5182.
[30] T.M. Abdel-Fattah, S. Ebrahim, M. Soliman, M. Shehab, Graphene Quantum Dots as Optical Sensor for Glucose Detection, MA2016-02 2016 3782.
[31] D.C. Marcano, D.V. Kosynkin, J.M. Berlin, A. Sinitskii, Z. Sun, A. Slesarev, L.B. Alemany, W. Lu, J.M. Tour, Improved synthesis of graphene oxide, ACS Nano 4 (2010) 4806–4814.
[32] D. Pan, J. Zhang, Z. Li, M. Wu, Hydrothermal route for cutting graphene sheets into blue-luminescent graphene quantum dots, Adv. Mater. 22 (2010) 734–738.
[33] S. Kim, D.H. Shin, C.O. Kim, S.S. Kang, S.S. Joo, S.-H. Choi, S.W. Hwang, C. Sone, Size-dependence of Raman scattering from graphene quantum dots: interplay between shape and thickness, Appl. Phys. Lett. 102 (2013), 053108.
[34] Y. Liu, C. Deng, L. Tang, A. Qin, R. Hu, J.Z. Sun, B.Z. Tang, Specific detection of d-glucose by a tetraphenylethene-based fluorescent sensor, J. Am. Chem. Soc. 133 (2011) 660–663.
[35] Y. Hong, J.W.Y. Lam, B.Z. Tang, Aggregation-induced emission: phenomenon, mechanism and applications, Chem. Commun. (2009) 4332–4353.
[36] Z. Zhao, Z. Wang, P. Lu, C.Y.K. Chan, D. Liu, J.W.Y. Lam, H.H.Y. Sung, I.D. Williams, Y. Ma, B.Z. Tang, Structural modulation of solid-state emission of 2,5-bis (trialkylsilylethynyl)-3,4-diphenylsiloles, Angew. Chem. 48 (2009) 7608–7611.